Supplemental figures

Name	Mutations	Selection
Triple$^{APC\text{WT}}$	$KRAS^{G12D}$, $P53^{KO}$, $SMAD4^{KO}$	-EGF, +nutlin-3, -noggin
Triple$^{P53\text{WT}}$	$KRAS^{G12D}$, APC^{KO}, $SMAD4^{KO}$	-EGF, -Wnt, -R-spondin, -noggin
Triple$^{SMAD4\text{WT}}$	$KRAS^{G12D}$, APC^{KO}, $P53^{KO}$	-EGF, -Wnt, -R-spondin, +nutlin-3
Triple$^{KRAS\text{WT}}$	APC^{KO}, $P53^{KO}$, $SMAD4^{KO}$	-Wnt, -R-spondin, +nutlin-3, -noggin
Quadruple	$KRAS^{G12D}$, APC^{KO}, $P53^{KO}$, $SMAD4^{KO}$	-EGF, -Wnt, -R-spondin, +nutlin-3, -noggin

Table S1. Overview of the generated mutants and the functional selection strategies used to select. The first column depicts the names of the mutants as used throughout the manuscript.

SAMPLE	CHR	POS	ID	MUT	VAF	TYPE	GENE	ENSEMBL_ID	AA_CHANGE
Quadruple t=0	1	79107484	1:79107484_C/A	C>A	0.333333333333333	missense_variant	IFI44L	ENSG00000137959	p.Pro450His
	2	27804714	2:27804714_T/C	T>C	0.230769230769231	missense_variant	C2orf16	ENSG00000221843	p.Cys1759Arg
	2	241696797	COSM5085335	C>T	0.08	missense_variant	KIF1A	ENSG00000130294	p.Ala933Thr
	4	48996643	4:48996643_C/A	C>A	0.4375	missense_variant	CWH43	ENSG00000109182	p.Asp173Glu
	6	30917809	COSM4528845	G>A	0.1875	missense_variant	DPCR1	ENSG00000168631	p.Gly523Glu
	7	45025698	7:45025698_T/G	T>G	0.333333333333333	splice_acceptor_variant&intron_variant	SNHG15	ENSG00000232956	
	7	100349614	COSM3831308	T>C	0.222222222222222	missense_variant	ZAN	ENSG00000146839	p.Leu629Pro
	12	50746243	COSM940340	T>G	0.333333333333333	missense_variant	FAM186A	ENSG00000185958	p.Thr1458Pro
	12	116445443	12:116445443_T/A	T>A	0.333333333333333	splice_acceptor_variant&intron_variant	MED13L	ENSG00000123066	
Quadruple t=4	1	79107484	1:79107484_C/A	C>A	0.526315789473684	missense_variant	IFI44L	ENSG00000137959	p.Pro450His
	4	48996643	4:48996643_C/A	C>A	0.296296296296296	missense_variant	CWH43	ENSG00000109182	p.Asp173Glu
	5	178552086	COSM1721135	T>G	0.227272727272727	missense_variant	ADAMTS2	ENSG00000087116	p.Asn949Thr
	7	92099047	COSM4386366	A>G	0.130434782608696	missense_variant	ERVW-1	ENSG00000242950	p.Ser217Pro
	8	144378426	8:144378426_T/C	T>C	0.318181818181818	missense_variant	ZNF696	ENSG00000185730	p.Phe194Ser
	9	117085613	9:117085613_G/C	G>C	0.307692307692308	missense_variant	ORM1	ENSG00000229314	p.Gly67Ala
	11	1619423	COSM4190294	T>C	0.1875	missense_variant	KRTAP5-2	ENSG00000205867	p.Ser20Gly
	12	104378700	12:104378700_T/C	T>C	0.1	splice_donor_variant& intron_variant	TDG	ENSG00000139372	
	14	107083426	14:107083426_G/C	G>C	0.117647058823529	missense_variant	IGHV4-59	ENSG00000224373	p.Pro60Ala
	19	35863298	19:35863298_A/G	A>G	0.2	missense_variant	GPR42	ENSG00000126251	p.Asn346Ser
	21	45994014	COSM579461	C>T	0.142857142857143	missense_variant	KRTAP10-4	ENSG00000215454	p.Pro127Ser
Quadruple Metastasis	1	176709311	1:176709311_G/T	G>T	0.307692307692308	missense_variant	PAPPA2	ENSG00000116183	p.Gly1377Val
	7	92099047	COSM4386366	A>G	0.14	missense_variant	ERVW-1	ENSG00000242950	p.Ser217Pro
	9	72897347	9:72897347_A/C	A>C	0.592592592592593	missense_variant	SMC5	ENSG00000198887	p.Asn277His
	9	117085595	9:117085595_C/A	C>A	0.272727272727273	missense_variant	ORM1	ENSG00000229314	p.Ser61Tyr
	9	117085613	9:117085613_G/C	G>C	0.363636363636364	missense_variant	ORM1	ENSG00000229314	p.Gly67Ala
	14	77239560	COSM958066	C>A	0.46875	missense_variant	VASH1	ENSG00000071246	p.Pro179His
	15	32921952	15:32921952_C/T	C>T	0.101694915254237	missense_variant	ARHGAP11A	ENSG00000198826	p.Thr365Ile
	19	35863298	19:35863298_A/G	A>G	0.125	missense_variant	GPR42	ENSG00000126251	p.Asn346Ser
	19	41743987	COSM3892633	C>T	0.441860465116279	missense_variant	AXL	ENSG00000167601	p.Arg308Cys
	19	56663214	19:56663214_A/G	A>G	0.269230769230769	missense_variant	AC024580.1	ENSG00000204533	p.Ser13Pro
	21	45994014	COSM579461	C>T	0.25	missense_variant	KRTAP10-4	ENSG00000215454	p.Pro127Ser

Table S2. Whole genome sequencing of quadruple mutant organoids and derived metastasis do not show subclonal outgrowth *in vitro* and *in vivo*. Missense, nonsense and splice site mutations are depicted in quadruple mutant cultures at the time it was transplanted, after it was kept in culture for 4 months and of a resulting metastasis. No common driver mutations were found and the identified mutations all have a relatively low variant allele frequency (VAF), suggesting that additional mutations in the cells were not responsible for the metastatic phenotype.

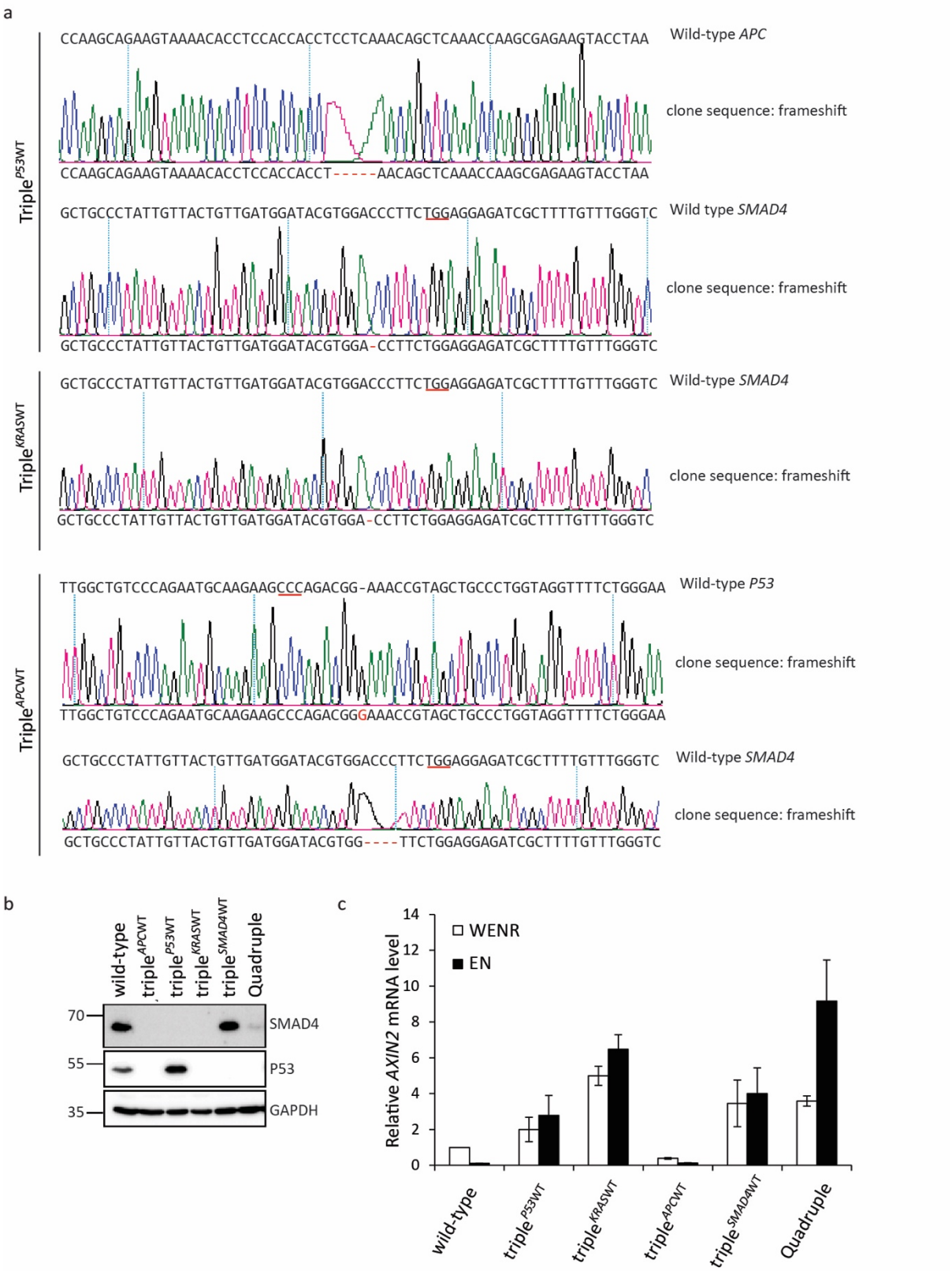
a
Triple P53WT
CCAAGCAGAAGTAAAACACCTCCACCACCTCCTCAAACAGCTCAAACCAAGCGAGAAGTACCTAA
Wild-type APC
clone sequence: frameshift
CCAAGCAGAAGTAAAACACCTCCACCACCT-----AACAGCTCAAACCAAGCGAGAAGTACCTAA
GCTGCCCTATTGTTACTGTTGATGGATACGTGGACCCTTCTGGAGGAGATCGCTTTTGTTTGGGTC
Wild type SMAD4
clone sequence: frameshift
GCTGCCCTATTGTTACTGTTGATGGATACGTGGA-CCTTCTGGAGGAGATCGCTTTTGTTTGGGTC
Triple KRASWT
GCTGCCCTATTGTTACTGTTGATGGATACGTGGACCCTTCTGGAGGAGATCGCTTTTGTTTGGGTC
Wild-type SMAD4
clone sequence: frameshift
GCTGCCCTATTGTTACTGTTGATGGATACGTGGA-CCTTCTGGAGGAGATCGCTTTTGTTTGGGTC
Triple APCWT
TTGGCTGTCCCAGAATGCAAGAAGCCCAGACGG-AAACCGTAGCTGCCCTGGTAGGTTTTCTGGGAA
Wild-type P53
clone sequence: frameshift
TTGGCTGTCCCAGAATGCAAGAAGCCCAGACGGGAAACCGTAGCTGCCCTGGTAGGTTTTCTGGGAA
GCTGCCCTATTGTTACTGTTGATGGATACGTGGACCCTTCTGGAGGAGATCGCTTTTGTTTGGGTC
Wild-type SMAD4
clone sequence: frameshift
GCTGCCCTATTGTTACTGTTGATGGATACGTGG----TTCTGGAGGAGATCGCTTTTGTTTGGGTC
b
wild-type
triple APCWT
triple P53WT
triple KRASWT
triple SMAD4WT
Quadruple
70
SMAD4
55
P53
35
GAPDH
c
Relative AXIN2 mRNA level
WENR
EN
0
2
4
6
8
10
12
14
wild-type
triple P53WT
triple KRASWT
triple APCWT
triple SMAD4WT
Quadruple

Figure S1. Generation of Triple^{KRASWT}, Triple^{APCWT} and Triple^{P53WT} mutant human colon organoids using CRISPR/Cas9. **(A)** PCR amplification products of the mutated alleles of *P53* and *SMAD4* in Triple^{APCWT}, *SMAD4* in Triple^{KRASWT} and *APC* and *SMAD4* in Triple^{P53WT}, were obtained using primers flanking the targeted exon (Drost et al., 2015). Subsequent sequencing revealed indels at the expected locations. PAM sequences are underlined in red in wild-type sequences. **(B)** Western blot analysis of SMAD4 and P53 expression in the indicated mutant human colon organoid lines, confirming the mutational status of the organoids. GAPDH, loading control. Please note the reduced SMAD4 expression in quadruple organoids, caused by the presence of a frameshift-inducing mutation in one allele and an in-frame deletion in the second allele (Drost et al., 2015). **(C)** Q-RT-PCR analysis for h*AXIN2* in the indicated organoid lines cultured in the presence (WENR) or absence (EN) of Wnt/R-spondin confirms inactivating mutations in *APC*. Expression was normalized to *GAPDH*. Mean and standard deviation of three independent experiments.

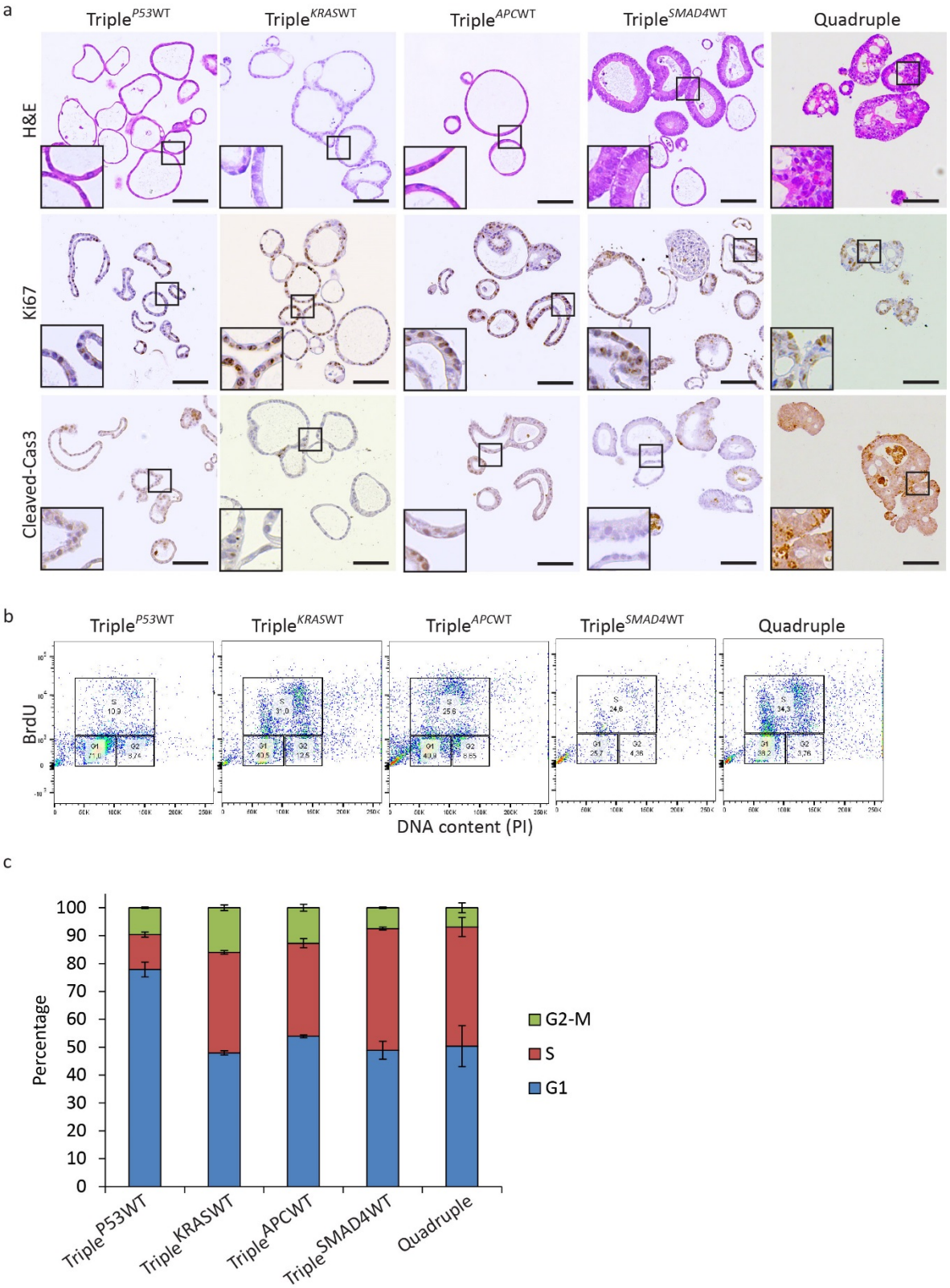
a
Triple P53WT
Triple KRASWT
Triple APCWT
Triple SMAD4WT
Quadruple
H&E
Ki67
Cleaved-Cas3
b
Triple P53WT
Triple KRASWT
Triple APCWT
Triple SMAD4WT
Quadruple
BrdU
DNA content (PI)
c
Percentage
100
90
80
70
60
50
40
30
20
10
0
G2-M
S
G1
Triple P53WT
Triple KRASWT
Triple APCWT
Triple SMAD4WT
Quadruple

Figure S2. *In vitro* characterization of mutant human colon organoids. **(A)** Representative H&E (top), Ki-67 (middle) and cleaved caspase-3 (bottom) immunostainings on the indicated mutant human colon organoid lines. Scale bars 100 μm. **(B)** Representative FACS plots of cell cycle profile analysis on the indicated mutant organoid lines. **(C)** Quantification of the cell cycle profile analysis in the indicated mutants. Represented are the percentages of cells in G1-, S- and G2/M-phase of the cell cycle. Average and SD of three independent experiments.

a Primary tumor

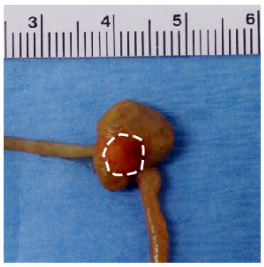

b Primary tumor

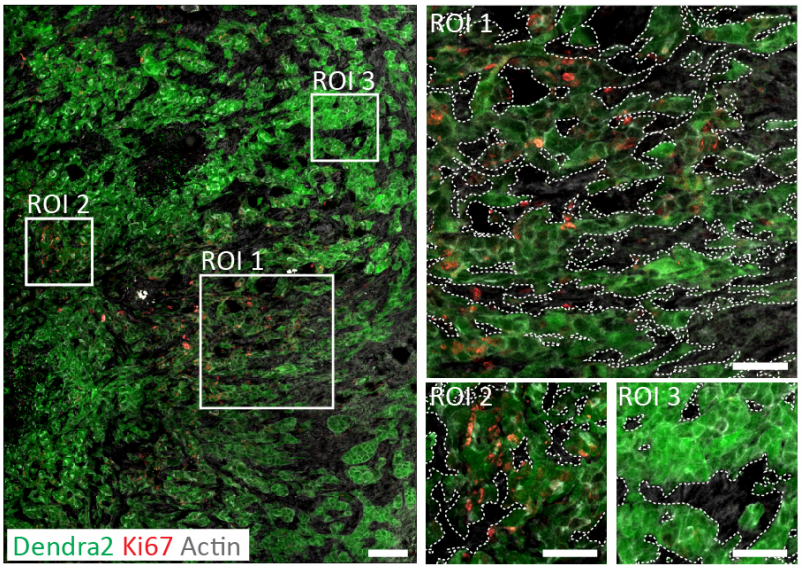

Figure S3. Development of an orthotopic intestinal organoid transplantation model to study CRC progression. **(A)** Representative picture of orthotopic primary tumor 8 weeks after organoid transplantation. Dashed lines highlight the tumor edges. **(B)** Immunofluorescence images of a primary tumor. The borders between tumors tissue and healthy tissue are indicated with a dotted line. Green represents tumor cells, red proliferative cells and gray all cells. Scale bars 100 μm, except ROI images in b, where scale bars represent 50 μm.

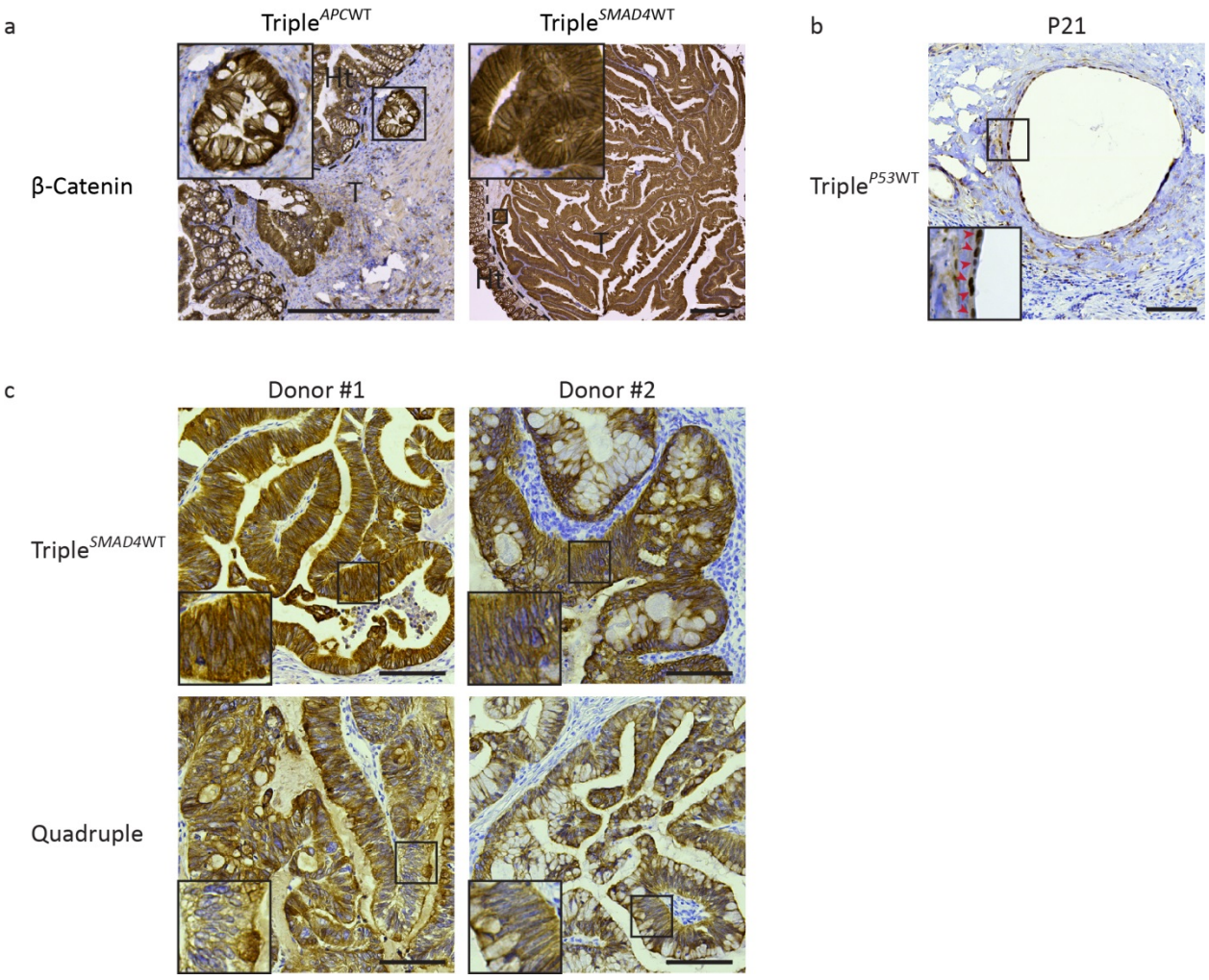

Figure S4. In-depth characterization of orthotopic human CRC. **(A)** β-Catenin staining on Triple$^{APC\text{WT}}$ and Triple$^{SMAD4\text{WT}}$ primary tumors. Dashed lines highlight tumor edges. T=tumor; Ht= healthy tissue. Scale bars 500µm. **(B)** P21 staining of a Triple$^{P53\text{WT}}$ primary tumor. Arrowheads point to P21 postive cells. Scale bar 100 µm. **(C)** CK7/8 staining of Triple$^{SMAD4\text{WT}}$ and Quadruple primary tumors obtained from two independent donors. Scale bars 100 µm.

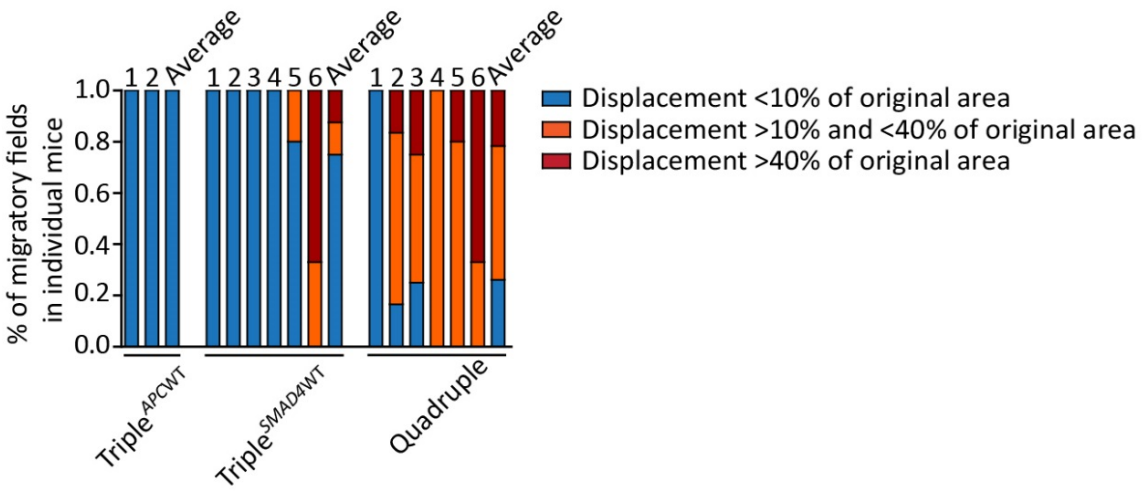

Figure S5. Classifciation of the migratory behavior of the different imaging fields in individual mice per each condition. See Figure 3C for the quantification.

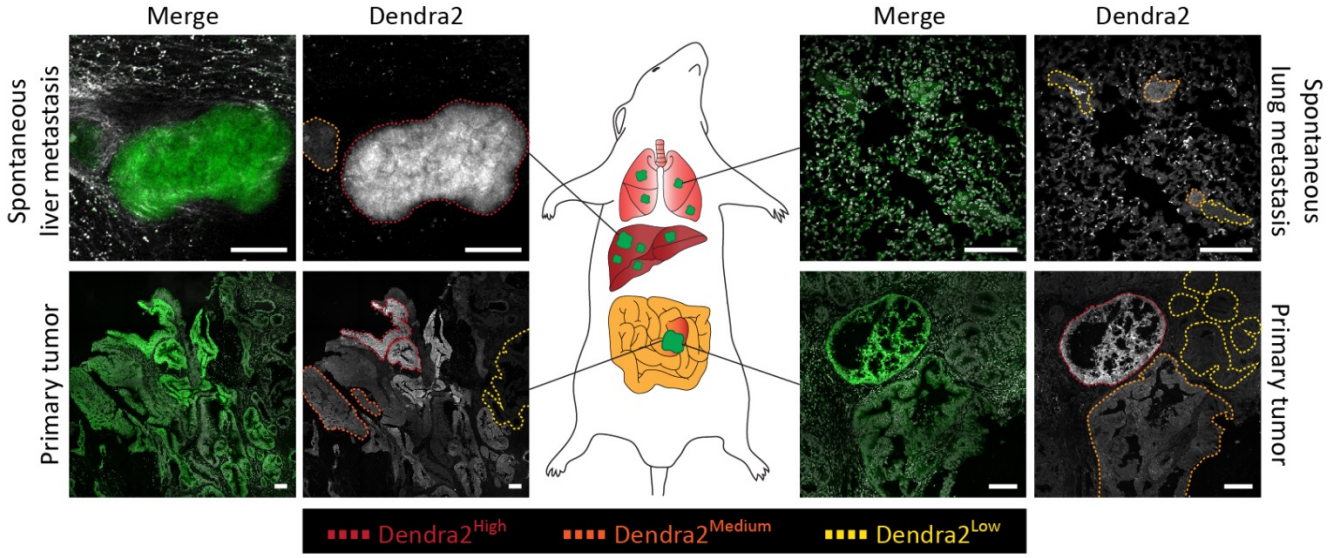
Merge
Dendra2
Merge
Dendra2
Spontaneous liver metastasis
Spontaneous lung metastasis
Primary tumor
Primary tumor
Dendra2High
Dendra2Medium
Dendra2Low

Figure S6. Clonal characterization of primary tumors and corresponding spontaneous metastases. Examples of confocal images of primary tumors and corresponding metastases originated from different clones present in the primary tumor. Representative clones with either high, medium or low expression level of Dendra2 are highlighted in red, orange and yellow respectively. Scale bars 100 μm.

a

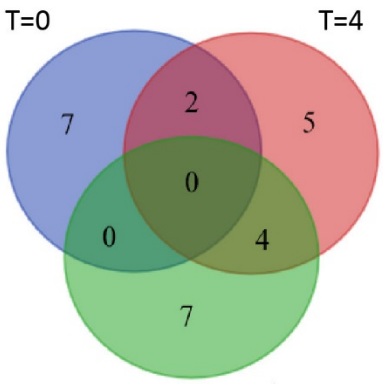
T=0
T=4
7
2
5
0
0
4
7
Spontaneous liver metastasis

b

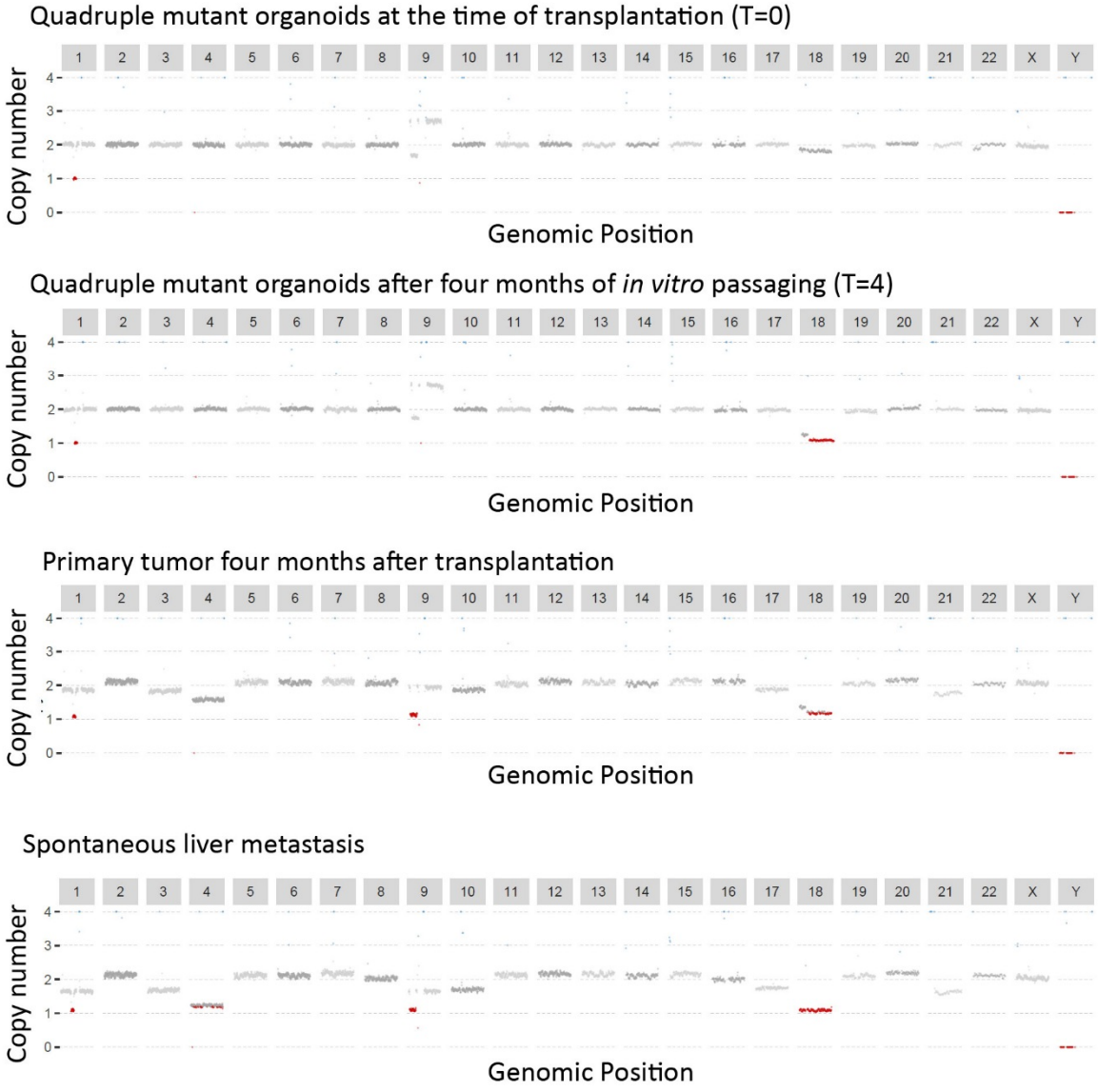
Quadruple mutant organoids at the time of transplantation (T=0)
Copy number
Genomic Position
Quadruple mutant organoids after four months of in vitro passaging (T=4)
Copy number
Genomic Position
Primary tumor four months after transplantation
Copy number
Genomic Position
Spontaneous liver metastasis
Copy number
Genomic Position

Figure S7. Mutation load analysis. Whole genome sequence analysis of quadruple mutant culture at the time it was transplanted, after it was kept in culture for 4 months and of a resulting spontaneous metastasis. **(A)** Venn diagram showing that many mutations are shared between the different samples, suggesting a common cause. **(B)** Each data point represents the GC corrected median copy number per 500 kb plotted over the genome with alternating colors per chromosome. Red regions indicate deleted regions and blue regions gains as detected by FREEC.

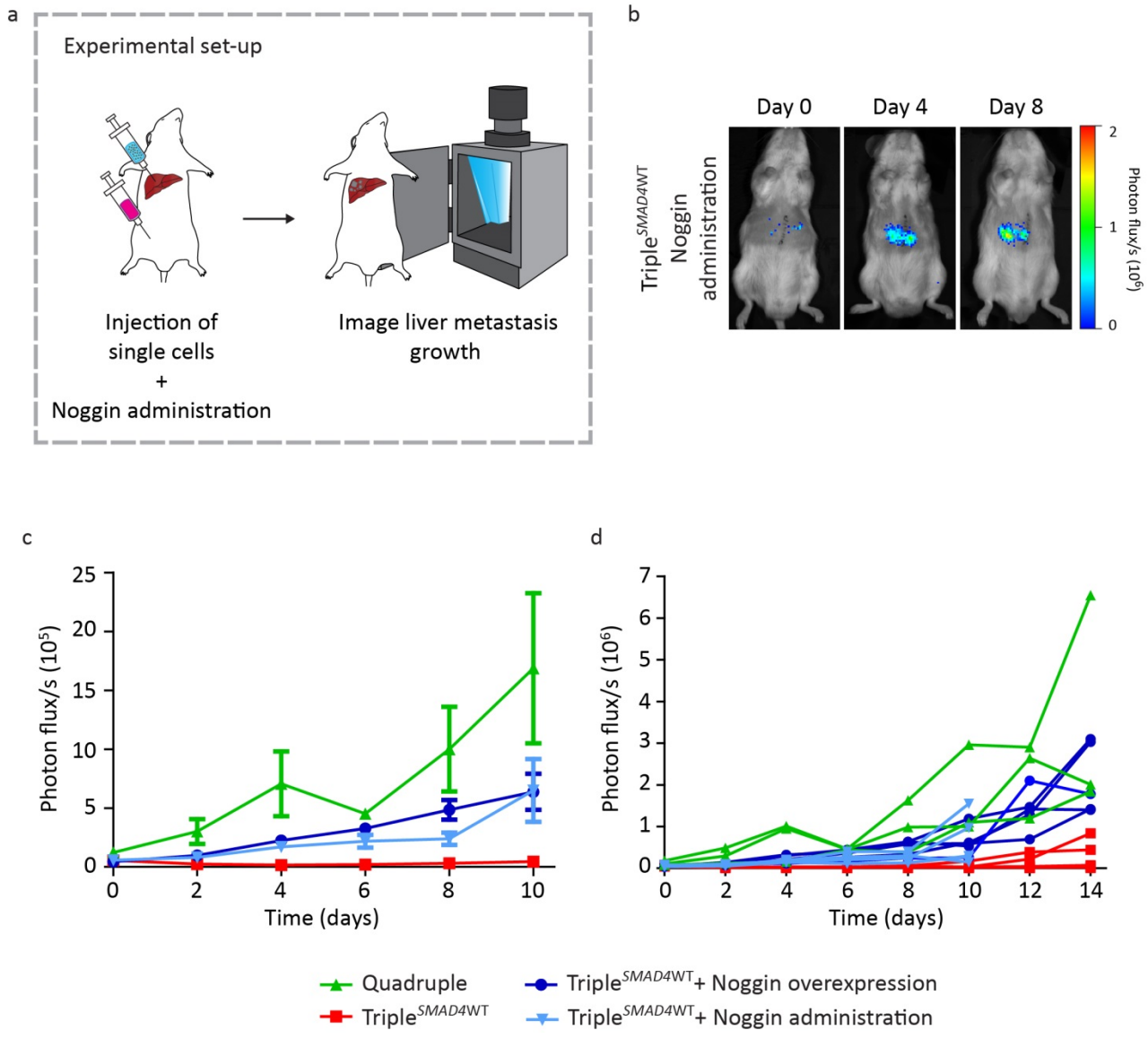
a
Experimental set-up
Injection of single cells + Noggin administration
Image liver metastasis growth
b
Day 0
Day 4
Day 8
Triple^SMAD4WT Noggin administration
Photon flux/s (10^6)
c
Photon flux/s (10^5)
Time (days)
d
Photon flux/s (10^6)
Time (days)
Quadruple
Triple^SMAD4WT
Triple^SMAD4WT + Noggin overexpression
Triple^SMAD4WT + Noggin administration

Figure S8. Metastatic growth upon reconstitution of the niche in individual mice.

(A) Mutant human colon organoids were dissociated and subsequently 50,000 cells were intrahepatically injected in mice. The niche was reconstituted by intraperitoneal injection of Noggin. Tumor growth was monitored by bioluminescence. **(B)** Representative images at indicated timepoints. (**C)** The kinetics of metastatic growth. Points are averages and error bars indicate SEM of biological replicates. Quadruple N=3, Triple$^{SMAD4\text{WT}}$, Triple$^{SMAD4\text{WT}}$ overexpressing Noggin N=5 and Triple$^{SMAD4\text{WT}}$ injected with Noggin N=5. **(D)** Kinetics of metastatic growth in individual mice of Figure 5 and S8B are shown.

a

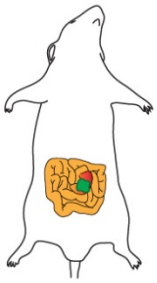

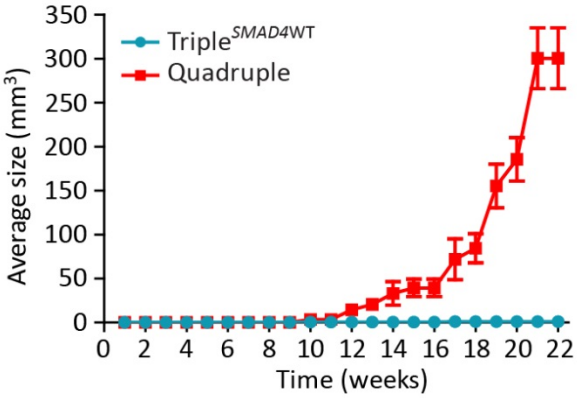

b

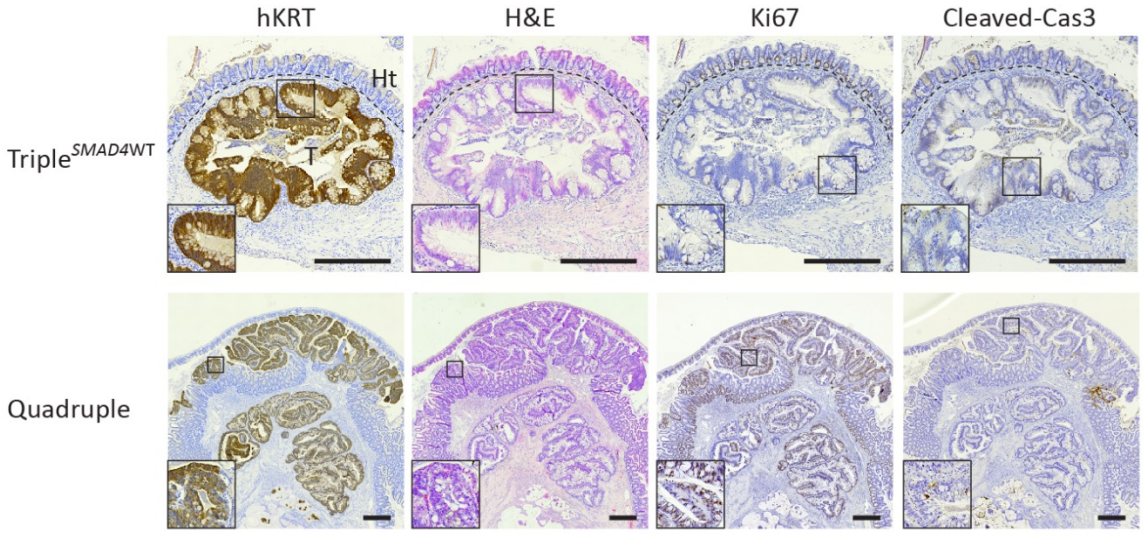

c

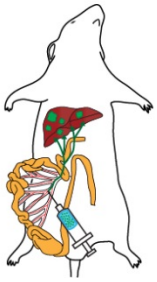

Metastatic capacity

	Mice with metastasis	Total number of metastasis	Metastatic load (mm^2)
Triple^{SMAD4WT}	0% (0/3)	0	-
Quadruple	67% (2/3)	3	3.36 E-01

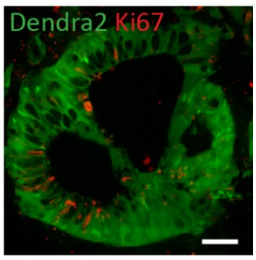

Figure S9. Validation of results in a second independent human colon organoid line. **(A)** Triple^{SMAD4WT} and quadruple mutation combinations were introduced in a second independent human colon organoid line and orthotopically transplantated. Graph represents the average tumor growth *in vivo*. Tumor volume was measured weekly by palpation. Error bars indicate the SEM of biological replicates. **(B)** Human-specific cytokeratin, H&E, Ki-67 and cleaved caspase-3 immunostainings on tumors isolated from mice transplanted with the indicated mutant human colon organoids. Scale bars 500 μm. **(C)** Mutant human colon organoids were dissociated and 250,000 cells were subsequently injected into a mesenteric vein of immune-deficient mice. After 6 weeks, livers were analyzed for the presence of metastases. Left, graph representing the number of formed metastases. Right, representative image of a quadruple mutant metastasis (green) stained for Ki67 staining (red). Scale bar 50 μm.

Supplemental References

Drost, J., van Jaarsveld, R. H., Ponsioen, B., Zimberlin, C., van Boxtel, R., Buijs, A., Sachs, N., Overmeer, R. M., Offerhaus, G. J., Begthel, H.*, et al.* (2015). Sequential cancer mutations in cultured human intestinal stem cells. Nature *521*, 43-47.